Sequential run of the PEO process with various pulsed bipolar current waveforms

Vitalios Ntomprougkidis, Julien Martin, Alexandre Nominé, G. Henrion

Sequential run of the PEO process with various pulsed bipolar current waveforms

V. Ntomprougkidis[1,2], J. Martin[1,2,*], A. Nominé[1,3], G. Henrion[1,2]

[1] Institut Jean Lamour – UMR 7198 CNRS – Université de Lorraine – 2 allée André Guinier, F-54011 Nancy, France

[2] Laboratoire d'Excellence Design of Alloy Metals for low-mAss Structures ('LabEx DAMAS') - CNRS - Université de Lorraine – 7 rue Félix Savart, F-57070 Metz, France

[3] Department of Nanophotonics and Metamaterials, ITMO University, St. Petersburg 197101, Russia

*Corresponding author: +33 383 584 251,julien.martin@univ-lorraine.fr

Highlights

- Behaviour of micro-discharges explained by a mechanism of charge accumulation.
- Coating growth rate and quality enhancement by sequential processing.
- Appearance of the beneficial soft regime is affected by sequential processing.
- PEO sequenced treatments open opportunities for energy reduction.

Graphical abstract

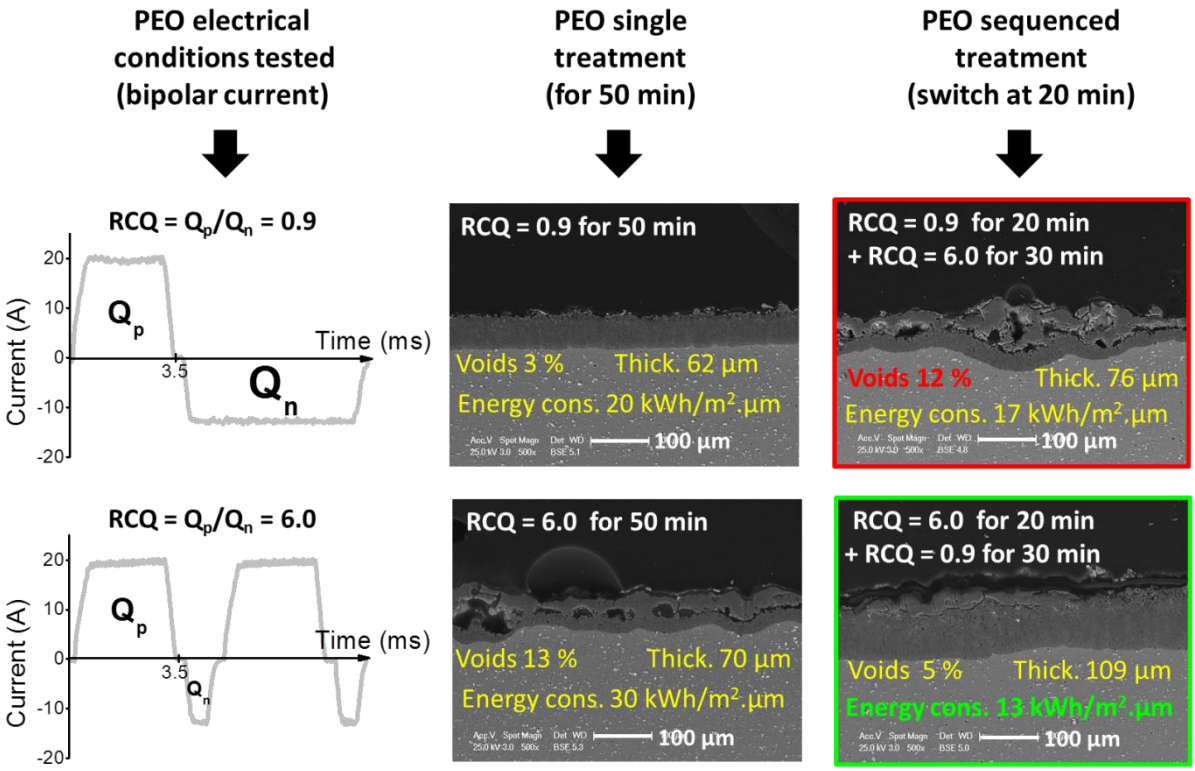

Abstract:

Oxide coatings were produced on a 2024 aluminium alloy using a pulsed bipolar current plasma electrolytic oxidation (PEO) process in an alkaline electrolyte. The use of sequences including various current waveforms during the same treatment was investigated, mainly by applying various combinations of two different anodic to cathodic charge quantity ratio (RCQ = 0.9 and 6.0). The morphology of the produced PEO coatings was observed using scanning electron microscopy while the behaviour of the micro-discharges was characterized in real time with the process using plasma diagnostic techniques. Compared with conventional treatments conducted in a single sequence, results evidenced that the thickness and the compactness of the PEO coating are enhanced by switching from a high to a low RCQ value in the course of the process. In contrast, reverse sequenced treatments leads to a significant deterioration of the produced PEO coating. A possible explanation exposed in the present study consists in considering the main role played by the mechanism of charge accumulation at the electrolyte / oxide interface on the micro-discharges behaviour with respect to the coating morphology and the applied charge quantity ratio. Finally, by establishing a relationship between process, physical and material quantities, this study demonstrate that the use of sequenced treatments open opportunities for a better energetic management of the PEO process.

Keywords: Plasma Electrolytic Oxidation (PEO); Micro-Arcs Oxidation (MAO); Pulsed bipolar current; Sequential treatment; Electrical Double Layer (EDL);

1. Introduction

Plasma electrolytic oxidation (PEO) is a surface engineering process suitable for lightweight metals (Al, Mg, Ti) and their alloys to form protective ceramic coatings [1]. Based on an electrochemical conversion of the metal surface, the rapid growth of the oxide layer takes place at high potential beyond the critical dielectric breakdown threshold of the growing insulating layer. This leads to the development of numerous tiny and short-lived micro-discharges (MDs) that move randomly over the processed surface [2-4]. When applied to aluminium alloys, the resulting PEO coatings exhibit improved hardness (1500 Hv) and wear resistance (1.10^{-4} $mm^3/N.m$). Indeed the index of crystallinity of the formed aluminium oxide remains close to 100% (amorphous in the case of conventional acid anodizing) including the presence of γ-Al_2O_3 and the $-\alpha Al_2O_3$ in various proportion [5, 6]. Moreover, as it uses diluted alkaline electrolytes free of any heavy metals or carcinogenic, mutagenic and reprotoxic (CMR) substances, the PEO process complies with the present environmental and health regulations. Therefore, it gains a growing interest in various domains (transport, energy, medicine, leisure and home) to replace conventional chromic or sulphuric acid anodizing processes. Despite these advantages, its deployment at the industrial scale remains still restricted due to relatively high costs arising from the use of high current densities (up to 10 - 100 A/dm^2) and high voltages (up to 400 – 1000 V) that renders the process highly energy consuming. In the literature, works devoted to improve the energy efficiency of the PEO process are abundant but two main approaches emerged.

Firstly, by adopting a process engineering approach, the main way that is explored consists in adjusting the PEO processing parameters, mainly the electrolyte composition [7-11] and the applied electrical signal [3, 4, 12-17]. On this last point, the electrical parameters play an important role in the process since they have a strong influence on both the space and time characteristics of the MDs, which affect in turn the final coating properties. On this point, it

has been established that the use of a pulsed bipolar current (PBC) to supply the electrodes results in a better quality of the coatings in terms of thickness and compactness [12,18]. Under this PBC mode, additional works have also found that the suitable adjustment of the waveforms of the current pulse, *i.e.* the anodic and cathodic current amplitudes, the pulse duration and the current frequency can determine the growth mode of the oxide films. Particularly, pioneer works from Jaspard-Mécuson *et al.* have shown that the right control of the charge quantity ratio $RCQ = Q_p / Q_n$ (ratio of positive Q_p to negative Q_n charge quantities applied during one period of the current pulse) is crucial and promotes the appearance of a particular growth regime called "soft" regime [3]. The appearance of this "soft" regime is mainly conditioned by maintaining a *RCQ* that must be set less than one, more specifically in the range between 0.8 and 1 [3,4,19]. This regime that occurs after a certain initial period of conventional PEO arcs regime is always associated with both a gradual decrease in the electrical voltage, a change in the optical emission due to the gradual disappearance of the MDs and a reduction in the acoustic noise [3]. It is also worth noting that despite the gradual disappearance of visible MDs during "soft" regime, advantages of PEO process are kept and some of them are emphasized (*e.g.* higher growth rate, higher proportion of high temperature crystalline phases, less large porosities). In addition, it was also established that the occurrence of this beneficial "soft" regime could happen earlier in the process by working with both a higher frequency and / or a higher current density leading therefore to a significant reduction in the specific electrical energy consumption (*i.e.* the electrical energy needed to grow 1 µm thick of compact oxide layer over 1 m^2 processed surface) [4].

The second approach, regarding the improvement of the energy efficiency of the PEO process, consists in getting a better understanding of the physicochemical mechanisms that govern the growth of the PEO oxide layers under an electrical discharge regime. Although advances have been made over the past few years in proposing phenomenological description

of what happens during the PEO process, growth mechanisms are still not well understood; clear relationship between the process parameters, the micro-discharge properties and the coating growth remains to be established as well. However, it is usually admitted that such growth mechanisms can be classified into two groups, those that describe the oxidations processes of the metal when submitted to an electrical discharge regime [20-25], and those that describe the dielectric breakdown processes of the insulating coating when surrounded with a cooled and a conductive liquid [26-32]. In the first group, on the basis of the steam and gas vial model, Klapkiv *et al.* [20, 21] suggested a single-discharge model with a core/shell structure. Later, Sundararajan *et al*. [22, 23] showed that the molten material, which is ejected through discharge channels, is oxidized, rapidly solidified and deposited on the surface, promoting thus the growth of the oxide layer. For Yerokhin *et al.* [24], two simultaneous mechanisms of the metal oxidation take place through the discharge channels including a plasma-assisted oxidation and an electrochemical-assisted oxidation. More recently, by using ^{18}O isotope tracers through PEO coatings, Matykina *et al.* [25] concluded that migration of oxygen is the result of two concomitant mechanisms, *i.e.*one by the solid-state diffusion of oxygen and another due to water molecules trapped in cavities which within the plasma decompose and form ions and radicals. For the second group of mechanisms, *i.e.* those that tend to explain the occurrence of the MDs at the metal surface during the PEO process, Hussein *et al.* [26-27] suggested a multi-discharge model including three types of discharges igniting at several locations and at different times through the coating thickness: A-type discharges that appear on the fine impurities located on the top surface of the coating, B-type discharges that cross the overall thickness of the coating, and C-type discharges that occur in the micro-sized porosities of the coatings. On the basis of optical emission spectroscopy measurements, Jovović *et al.* [28] were able to confirm these three types of discharges. Using a silicate-based electrolyte, Dehnavi *et al.* [29] established that A-type discharges are caused by the presence of silicon

anions adsorbed on the topmost surface of the growing oxide layer. Later, Cheng *et al.* [30-32] enriched Hussein's model by including D- and E-type discharges in order to explain the typical morphology of the PEO coatings, *i.e.* the presence of an outer porous sublayer filled with electrolyte and an inner dense sublayer. More recently, mechanisms involved in PEO treatments conducted under the specific "soft" sparking mode have been the subject of deeper investigations with a particular focus on the influence of the cathodic half-period in the ignition of MDs and coating growth [19, 33-35]. Indeed, if all studies agree with the fact the cathodic polarization is needed to prevent large and detrimental MDs, few works explain why this happens. Martin *et al.* evidenced that the appearance of the MDs is delayed with respect to the applied anodic current pulse, this delay being strongly influenced by the current waveform applied [19]. Considering the capacitive behaviour of the electrolyte / oxide system, authors assumed a phenomenological mechanism of anionic charge accumulation that takes place during the anodic alternation through the electrical double layer (EDL) located at the electrolyte / oxide interface until breakdown occurs. They also demonstrate that the magnitude of the cathodic current alternation influences mainly the dynamics of formation of the EDL (separated cationic H^+ and anionic OH^- species) during the subsequent anodic current alternation. Indeed, a significant excess in the cathodic current (ratio of charge quantity $RCQ << 1$) is associated to an excessive dispersion of anionic charges at the oxide / electrolyte interface and thus results in a longer anionic charge recharging process to restore the EDL during the subsequent anodic current. More recently, Nominé *et al.* considered the EDL thickness using Debye-Hückel's relation and the ion mobility in an alkaline silicate electrolyte (mainly K^+, Na^+, H^+ and OH^-). By varying the current pulse frequency, they estimated that anodic EDL requires ~200 µs to form. Considering a bipolar current pulse with 50% duty cycle, this corresponds to a frequency of ~2.5 kHz. [33]. At the same time, Rogov *et al.* suggested that the cathodic polarization is responsible of a reduction in the potential barrier through the EDL due to a local acidification

of the oxide – electrolyte interface that in turn reinforces the potential drop and the electric field at the metal / oxide interface during the subsequent anodic polarization. Based on this consideration, authors explained why, within "soft" regime conditions, it is possible to enhance anodic oxidation of the metal substrate and high-energy processes without strong discharges [34, 35].

The present study aims at contributing to a better understanding of the physical mechanisms that allow the coating growth under discharge regime while keeping in mind the necessity to decrease the energy consumption of the PEO process, as well as improving the produced coating quality. For this purpose, the main idea consists in investigating the PEO process by using sequential treatments with various set of electrical parameters, mainly by applying various RCQ to the electrodes. Particularly, two very different RCQ were considered in this work because they are known to result in opposite effects in terms of the produced PEO coating morphology and the electrical energy consumption. The first RCQ considered, RCQ = 6.0, allows to rapidly build up a thick but highly porous oxide layer – large open cavities - while the second RCQ, RCQ = 0.9, provides a thinner but a more compact coating with a substantial reduction in the energy consumption due to appearance of the "soft" regime in the course of the process [3, 4, 16]. By taking advantage of these two opposite electrical conditions within the same sequenced PEO treatments, it may be expected to achieve a synergetic effect which could results in the elaboration of improved PEO coatings performance with a significant energy gain. The effects of a sudden modification of the electrical conditions in the course of a PEO process is closely investigated and discussed by taking into account the correlation between several criteria based on the process monitoring data (voltage- and current-time responses), the MDs behaviour (light emission, surface density, spatial distribution and size) and the material characterization (thickness, porosity and element composition). Comparisons

with results collected from reference treatments run within a single sequence are also considered for discussion.

2. Material and experimental procedure

Sample made of Al2024 aluminium alloy (3.8 - 4.9 at. % Cu, 1.2 – 1.8 at. % Mg, 0.3 – 0.9 at. % Mn and Al as balance) were PEO processed in a solution of potassium hydroxide ([KOH] = 1 $g.L^{-1} \cong 0.018$ $mol.L^{-1}$) and anhydrous sodium silicate ([Na_2SiO_3] = 1.65 $g.L^{-1} \cong 0.014$ $mol.L^{-1}$) diluted in deionized water. The electrical conductivity and pH values are 2.8 $mS.cm^{-1}$ and 12.5, respectively. The composition of the electrolyte remained unchanged for all the treatments, its influence on the PEO process was not the subject of the present study. A cooling device allows keeping the electrolyte temperature at about 30 °C. Two rectangular titanium counter-electrodes (200 × 200 × 1 mm^3 in size) face both sides of the processed aluminium sample (50 × 30 × 6 mm^3 in size). The electrode gap between each titanium counter-electrode and the working aluminium sample is fixed at 90 mm.

PEO treatments were conducted by applying bipolar current to the electrodes. The use of a current controlled power supply makes it possible to optimally set and control the anodic and the cathodic currents amplitude, and therefore to control the respective charge quantities delivered to the electrolyser system. Various sequential PEO treatments were performed by changing the value of the charge quantity ratio (RCQ) during the process. It is worth noting that the two RCQ values considered in this study were set by adjusting only the waveform of the cathodic current pulse, while maintaining the anodic one unchanged. Values of current pulse magnitude, duration, frequency, and charge quantity are given in Table 1 together with a sketch of the current waveform for the RCQ values considered here. For all the sequenced

treatments investigated, the samples were systematically processed for 20 min with a first RCQ value. At 20 min processing, the current supply was switched to the second RCQ value without stopping the PEO treatment. Process continued with this second RCQ value for 30 min. Consequently, the total duration of all the sequential PEO treatments investigated was equal to 50 min. In parallel, and for comparison reasons, four reference treatments were also conducted that consist of single PEO treatment runs with the same RCQ values for 20 and 50 min (See Table 2).

Voltage and current waveforms were recorded at periodic intervals during the process using a 1 GHz bandwidth oscilloscope (Agilent 54832B). The light emitted by the micro-discharges (MDs) was detected with a photomultiplier (Hamamatsu R928), over the full range of visible spectrum. The recorded signal hence corresponds to a wavelength-integrated value. The output signal was amplified by a 300 MHz bandwidth current amplifier (Stanford Research Systems SR445) and recorded together with the current and voltage signals. As a complement, by using a high speed camera (Photron SA1.1), video recordings of the MDs were precisely conducted at time when the transition from the first RCQ to the second one occurs. Only the lower part of the sample is filmed over an area of 5.4 cm^2 (30 × 18 mm^2) providing a spatial resolution of 0.015 mm^2/pixel, which is at least three times lower than the average area of MDs that were detected in the experiments. The acquisition rate was fixed at 150 000 frames per second that corresponds to a time resolution of 6.6 µs. Image processing was performed using the home-developed TRACE software [36, 37]. It makes it possible to discriminate MDs from noise and to characterize their behaviour in the course of the treatment (spatial distribution, density and size).

X-ray diffraction (XRD) measurements were performed for the phase identification of the produced oxide coatings. A Bruker D8 ADVANCE diffractometer (Cu-K_α , λ=1,5406 Å) was used in θ/2θ Bragg-Brentano configuration with a step of 0.02 ° over a range from 20 ° to 80

°. The grown layers were observed by scanning electron microscopy (FEG-SEM Philips XL30). Prior to their observation, the samples were cut, mounted in resin and polished successively with various grades of SiC abrasive papers. A final step polishing was performed with a 1µm diamond paste. Observation of the coating cross-section was performed in back-scattered electron mode (25 kV accelerating voltage) while observation of the coating top-surface was conducted in secondary electron mode (5 kV accelerating voltage). Estimations of the thickness and the void fraction of the coating were conducted on cross-section SEM micrographs by using image processing that discriminates the coating from the substrate and the surrounding molding resin. The thickness and the fraction of voids were determined as the average values of 10 measures taken on cross-section over 10 different positions (each 500 µm). Moreover, it is necessary to clarify that voids correspond to cavities throughout the coatings that are larger than 1 µm in diameter, finer porosities being not detected after image processing. Finally, the chemical composition and the distribution of elements in the synthesized oxide layers were determined by EDX analyses on sample cross-sections.

3. Results

3.1 Establishment of the “soft” regime

Fig. 1 shows the time evolution of the anodic voltage amplitude for the different sequenced treatments investigated as well as for the associated reference treatments consisting of a single sequence.

At the beginning of the process, all curves reveal a quite similar trend with a strong increase in the voltage amplitude. During this early stage that only lasts for a few seconds**,** an initial amorphous oxide thin film grows with no visible micro-discharges (MDs) while a bluish luminescence and an intense gas release are visible all over the sample surface [27]. The point

at which the slope of the voltage curves significantly reduces (at about 620 V) is commonly designated as the dielectric breakdown voltage of the formed oxide layer. Once this specific voltage value is reached, the ignition of small blue-white MDs starts over the processed surface [7, 15, 30]. Until the switching point that will occur at 20 min, Fig. 1 shows that the anodic voltage amplitude follows a much reduced increase rate and the visible MDs become fewer and larger and they gradually turn into orange-red colour. It can also be noticed that during this stage, the anodic voltage amplitude reveals slight differences depending on the electrical conditions applied. Right before 20 min, the anodic voltage reaches 726 ± 5 V for the treatment performed with the low RCQ (RCQ = 0.9) while it reaches 755 ± 5 V for the treatment performed with the high RCQ (RCQ = 6.0).

Right after 20 min, a significant voltage drop is observed for the treatment that switches from the high RCQ to the low one while a slight voltage jump is noted for the reverse sequence. Particularly for the first, the anodic voltage decreases suddenly from 755 ± 5 V to 540 ± 10 V over less than 5 s following the transition, then increases for a period of 3 min and finally decreases with a much lower rate to stabilize at about 558 ± 10 V until the end of the treatment. For this specific sequence treatment, it is also worth noting that from the switching time at 20 min to the end of the process at 50 min, the anodic voltage amplitude constantly remains lower than all the other PEO treatments investigated. Additionally, Fig. 1 shows that the time at which the anodic voltage gradually decreases – usually referred to as the time of the "soft"-regime appearance and noted t_{SR} in Table 1- occurs earlier for this specific sequenced treatment (t_{SR} = 23 ± 1 min) than for the single reference treatment conducted with the low RCQ only (t_{SR} = 30 ± 1 min).

3.2 Delay in micro-discharges occurrence

Chronograms in Fig. 2 show the variations of the light emission, the current and the voltage over one pulse period of the current (10 ms) for the two sequenced treatments investigated and at different processing times *e.g.* after starting the process at 5 min, right before the switching point at 19 min 55 s, right after the switching point at 20 min 05 s and at the end of the process at 49 min 55 s.

Concerning the light emission, and as usually encountered under the processing conditions used in this study, light is only detected during the anodic polarization since MDs only appear during the anodic alternation of the current pulse [16, 33, 38]. Chronograms also evidence that the detected light is more or less delayed with respect to the rising edge of the anodic current pulse. In parallel with these chronograms, Fig. 3 reports the evolution of this delay (noted Δt) as a function of the processing time for each PEO treatment carried out. At the beginning of the process (at 1 min), and irrespective of the investigated conditions, the delay Δt is quite negligible (less than 10 µs) which means that MDs appear quite simultaneously with the applied anodic current. Until the switching point that will occur at 20 min, Fig. 3 shows that the delay gradually increases with the processing time. It increases more rapidly using the low RCQ (RCQ = 0.9) than the high one (RCQ = 6.0). Right before 20 min (at 19 min 55 s), the delay is long and reaches 1.19 ± 0.01 ms for the treatment performed with the low RCQ while it remains short and reaches only 0.14 ± 0.01 ms for the treatment conducted with the high RCQ.

Right after 20 min, Fig. 3b clearly puts in evidence that the delay Δt suddenly changes in different proportions depending on the sequenced treatment used. When switching from the low RCQ to the high one, the delay Δt instantaneously drops from 1.19 ± 0.01 ms to about 0.02 ± 0.01 ms. More interestingly, the delay Δt reached right after the switching time is largely lower than the delay measured at the same processing time with the corresponding reference

treatment conducted with the high RCQ only (Δt = 0.14 ± 0.01 ms). The opposite behavior is strictly observed for the reverse sequenced treatment. Indeed, when the process switches from the high RCQ to the low one, the delay Δt suddenly jumps from 0.14 ± 0.01 ms to 1.62 ± 0.01 ms. Similarly, it is also worth noting that the delay Δt reached right after the switching time is largely higher than the delay Δt measured at the same processing time with the corresponding reference treatment conducted with the low RCQ only (Δt = 1.19 ± 0.01 ms).

Finally, after a certain period of time following the switching time - from a few to tens of minutes depending on the sequenced treatment used - Fig. 3a shows that the delay in the MDs appearance tends to converge and to recover the value that it would have attained by using the corresponding reference treatment.

3.3 Time constant of the anodic voltage-time responses

Concerning the voltage-time response recorded over one pulse period of the anodic current, chronograms in Fig. 2 show that the voltage signal exhibits a transient regime during the first milliseconds following the beginning of the anodic pulse. The duration of this transient regime may be short or long, depending on the applied electrical conditions. As reported in a previous study, the experimental data of the anodic voltage-time response were adequately fitted by an exponential function giving access to the time constant of this transient regime [19]. In parallel with these chronograms, Fig. 4 reports the evolution of this time constant (noted τ) as a function of the processing time for each PEO treatment performed. At the beginning of the process (at 1 min), and irrespective of the investigated conditions, the time constant τ is low (less than 0.1 ms). Until the switching point that will occur at 20 min, Fig. 4 shows that the time constant gradually increases with the processing time. It increases more rapidly using the low RCQ (RCQ = 0.9) than the high one (RCQ = 6.0). Right before 20 min (at 19 min 55 s), the time

constant τ is long and reaches 0.43 ms for the treatment performed with the low RCQ while it remains short and reaches only 0.16 ms for the treatment conducted with the high RCQ. In addition, it is also worth noting that the evolutions of the delay Δt (Fig. 3) and the time constant τ (Fig. 4) for the different RCQ investigated are similar which is in good agreement with previous observations [19].

Right after 20 min, Fig. 4b evidences that the time constant τ suddenly changes in different proportions depending on the sequenced treatment applied. When switching from the low RCQ to the high one, the time constant τ behaves like the delay Δt in the MDs appearance since it suddenly drops from 0.43 ms to about 0.09 ms. Interestingly, the time constant τ reached right after the switching time is significantly lower than the time constant measured at the same processing time with the corresponding reference treatment conducted with the high RCQ only (τ = 0.16 ms). In addition and as already observed for the delay Δt, the opposite behaviour is strictly observed for the reverse sequence. Indeed, when the process switches from the high RCQ to the low one, the time constant suddenly jumps from 0.16 ms to 1.06 ms. For this specific sequenced treatment, the time constant τ reached right after the switching time is largely higher than the time constant τ measured at the same processing time with the corresponding reference treatment conducted with the low RCQ only (τ = 0.43 ms). Finally, Fig. 4 evidences that after a certain period of time following the switching time - from a few to tens of minutes depending on the sequenced treatment used - the time constant of the voltage-time response tends to converge and to recover the value that it would have attained by using the corresponding reference treatment.

3.4 Micro-discharges properties

Fig. 5 shows the evolutions of the MDs characteristics (surface density and average size) exactly at the time when the process switches from one RCQ to the second one. Fig. 5a is associated to the sequenced treatment that switches from the low RCQ (RCQ = 0.9) to the high RCQ (RCQ = 6.0) while Fig. 5b corresponds to the reverse sequence. Right before the switching point that will occur at 20 min, MDs exhibit the same behaviour as that already encountered in previous works *e.g.* numerous and small MDs are promoted with the low RCQ while the high RCQ results in less numerous and bigger MDs [4, 16, 19]. In addition, and as mentioned above concerning detection of the light emitted from the processed samples, Fig. 5 confirms that occurrence of the MDs is delayed with respect to the anodic current pulse, this delay remaining higher for the high RCQ.

Right after 20 min, when the processes enter into the new RCQ, Fig. 5 evidences that transition is associated with a sudden change in the MDs behaviour. Indeed, when the process switches from the low RCQ to the high one, both the surface density and the average size of the MDs suddenly increase from 6.5 $mm^{-2}ms^{-1}$ to 10.5 $mm^{-2}ms^{-1}$ and from 0.057 mm^2 to 0.091 mm^2, respectively. The opposite behaviour is strictly observed for the reversed sequence since both the surface density and the average size of the MDs suddenly decrease from 1.12 $mm^{-2}ms^{-1}$ to 0.28 $mm^{-2}ms^{-1}$ and from 0.105 mm^2 to 0.022 mm^2, respectively. Said differently, numerous and large MDs are promoted by switching from the low RCQ to the high one in the course of the process while less numerous and smaller size MDs are promoted with the reverse sequence.

3.5 Morphology of the produced PEO coatings

Figure 6 demonstrates XRD patterns of the produced oxide layers. Analysis of these patterns shows that the coatings were mainly composed of α- and γ-phases of alumina. In addition, it is seen that the relative intensity of peaks corresponding to α-phase is largely

increasing with respect to γ-phase when high charge ratio is involved in the process, i.e. single treatment with RCQ=6.0 and sequenced treatments. Moreover, transitional δ-phase was observed, which also exhibited an increase in these cases. These findings are consistent with the existing literature [13]. SEM micrographs in Fig. 7 compare the top-surface views of the different PEO coatings produced in the present study. All surfaces exhibit the typical morphology of the PEO coatings consisting in "pancake"-like structures with voids of about 1 - 100 µm in diameter. These voids are usually associated with discharge channels that take place during the PEO process [6, 12, 16]. This is particularly obvious for the oxide layer grown for 20 min under the high RCQ which exhibits a "crater"-like structure with large voids up to 10 µm in diameter. In contrast, the use of the low RCQ for 20 min results in the formation of a "sponge"-like structure with fine open pores less than 1 µm in diameter. After 50 min processing time, these differences are much more pronounced. Moreover, Fig. 7 also shows that the implementation of sequenced treatments has a significant effect on the morphology of the top-most surface compared to the associated reference treatments. Interestingly, by switching from the low RCQ to the high one, the fine "sponge-like" structure observed at 20 min turns into a rough "crater"-like structure at 50 min. The opposite morphological transformation is strictly observed for the reverse sequence.

SEM micrographs in Fig. 8 shows the cross-sectional views of the different PEO coatings produced in the present study. Moreover, and from a general point of view, the synthesized oxide layers exhibit the typical morphology of PEO coatings consisting in two distinct regions, more or less dependent on the processing conditions: a thick compact inner sublayer adjacent to the aluminium substrate and a highly porous outer sublayer with large cavities. In parallel with these cross-sectional views, Fig. 9 reports both the overall thickness of the oxide layer (thickness of the inner and the outer sublayers) and the fraction of voids (up to 1 µm in diameter) for the treatments carried out for 50 min. Concerning the reference treatments, the

use of the high RCQ results in a thick overall coating (70 ± 5 µm) with large cavities through the outer sublayer (void fraction 13 ± 3 %) while the used of the low RCQ leads to a slightly thinner coating (62 µm ± 5 µm) much more compact (void fraction ~ 3 ± 3 %). Moreover, and as already observed from the top-surface views, Fig. 8 and Fig. 9 also put in evidence that the use of sequenced treatments affect the final cross-sectional morphology of the coatings compared to the associated reference treatments. The sequence treatment involving the transition from the low RCQ to the high one has a detrimental effect on the morphology of the oxide layer. Indeed, although the overall thickness slightly increases (76 ± 5 µm), the fraction of voids significantly increases (12 ± 3 %) due to the presence of large cavities throughout the thickness. In contrast, the reverse sequence has a beneficial effect on the morphology of the oxide layer since the overall thickness significantly increases (~ 109 ± 5 µm) while maintaining a low fraction of voids (~ 5 ± 3 %).

Fig. 10 compares the EDX element maps recorded on the cross-section of the samples processed with the reference treatments performed for 50 min and with the specific sequenced treatment (RCQ = 6.0 for 20 min followed by RCQ = 0.9 for 30 min) that provides the thickest coating with a compact morphology. Whatever the applied conditions, the oxide layers mainly contain Al, O, Si and K elements. Al comes from the Al2024 aluminium alloy substrate while O, Si and K come from the electrolyte. EDX maps also evidence that Si and K species are preferentially located throughout the outer porous sublayer while the inner sublayer is mainly composed of Al and O. This observation is consistent with previous studies that also evidenced that open cavities, in contact with the electrolyte, incorporate elements from the electrolyte [39-41]. Nevertheless, some differences in the element distribution throughout the oxide layer are significant when comparing the different treatments investigated. In the case of the reference treatment conducted with the low RCQ, Si and K are quite evenly distributed throughout the outer sublayer, which is not the case for the reference treatment performed with

the high RCQ. In the specific case of the sequenced treatment that switches from the high RCQ to the low one, Si and K seem to be more concentrated and they are homogeneously distributed throughout a thicker outer sublayer, which could certainly provide a better corrosion protection of the aluminium alloy substrate. Indeed, some works that carried out PEO processes of aluminium in electrolyte with various amount of diluted silicate have established that the presence of such a silicon-rich barrier layer, mainly made of an amorphous silica SiO_2 or alumino-silica phase $3(AlO_3)\cdot 2(SiO_2)$, improve both wear resistance and the corrosion resistance of the aluminium alloys [39-41]. On that point, further corrosion experiments, mainly conducted via electrochemical impedance spectroscopy, should be devoted to verify a potential enhancement of the corrosion resistance of the samples processed with sequenced treatments, especially the one that switches from the high to the low RCQ.

4. Discussion

The present discussion focuses on the explanation of the experimental results by establishing relationship between the optical characterization of the micro-discharges, the morphological characterization of the produced PEO coatings and the various applied electrical conditions. In particular, making more explicit the link between the delay Δt in the MDs appearance, the time constant τ of the voltage-time response and the MDs properties is needed first to a better understanding of the key role played by the MDs on the morphology of the growing oxide layers. Finally, on the basis of the combined experimental results, the interest in using PEO sequenced treatments will be discussed from the point of view of the energy consumption.

4.1 Mechanism of charge accumulation

The schematic diagram in Fig. 11 shows the proposed mechanism of charge accumulation that could explain the relationship between the delay Δt in the MDs appearance, the time constant τ of the voltage-time response and the MDs properties, especially when the process suddenly switches from one RCQ to the second one in the course of the PEO treatment.

At the beginning of the process, results have shown that the delay in the MDs appearance - correlated to the time constant of the voltage-time response – gradually increases with the processing time (Fig. 3 and Fig. 4). It also increases more rapidly using the low RCQ than the high one. It was previously established that the ratio of charge quantity controls the dynamic of establishment of a stable electrical double layer (EDL) at the electrolyte / oxide interface, which in turn, once established, governs the dielectric breakdown of the oxide layer and therefore the ignition of the MDs [19]. The dynamic of establishment of this EDL is mainly affected by the mechanism of charge accumulation taking place at the interface between the oxide and the electrolyte. Depending on the substrate bias polarization, charges (cations (H^+) and anions (OH^-) that are expected to be the most important species in terms of number density and mobility) are accumulated at this interface during the anodic alternation of the current pulse while they are relaxed during the cathodic one. When processing with high RCQ (RCQ = 6.0) value, the low magnitude of the cathodic part (i.e. the combined effects of a low cathodic current amplitude and/or a short duration resulting in a low cathodic charge quantity) doesn't allow the complete relaxation of charges accumulated during the previous anodic alternation of the current. So, charges remain close to the interface and they accumulate much more rapidly during the subsequent anodic alternation. It results that the time needed to accumulate charge is short and breakdown occurs earlier with a short delay between the applied anodic current and the MDs appearance. It gives rise to large and long-lived MDs. In contrast, with the low RCQ - the amplitude of the cathodic current and the cathodic part duration being higher compared to the high RCQ – charges accumulated during an anodic alternation are highly

relaxed during the subsequent cathodic alternation and the accumulation mechanism restarts at each new anodic alternation. It results that the time needed to accumulate charge is long and breakdown occurs later with a long delay between the applied anodic current and the MDs appearance. In this case, it gives rise to small and short-lived MDs. Moreover, the fact that both the delay in the MDs appearance and the time constant of the voltage-time response gradually increase with the processing time is explained by taking into account some evolutions in the morphological aspects of the growing oxide layer, particularly its gradual thickening and the development of fine porosities, the latter exhibiting a higher specific area and a higher charge storage capacity. As the process goes on, more accumulated charges are therefore needed to reach the dielectric breakdown voltage of the growing oxide layer resulting in a longer delay Δt and in a longer time constant τ.

Right before the switching point, although the oxide layer elaborated with the low RCQ remains quite compact - no large cavities up to 10 µm in diameter are visible throughout the thickness -, SEM observations have revealed the presence of a fine "sponge"-like structure with very small porosities less than 1 µm in diameter at the top-most surface (Fig. 7). This sponge-like structure exhibits a high specific area associated with a high charge storage capacity. In this case, right before the switching point, the accumulation of charges at the oxide / electrolyte interface is therefore mainly limited due to two joint effects *e.g.* the application of a low RCQ (high extraction of electric charges during the high magnitude of the cathodic regime) to a "sponge"-like top-most surface (high dispersion of charges through the fine porosities filled with the conductive electrolyte) (Fig. 11a). This explains why, right before the switching point, the delay in the MDs appearance and the time constant of the voltage-time response reached high values (Fig. 3 and Fig. 4). It is also in good agreement with experimental results on the MDs behaviour which are numerous and but with small size (Fig. 5) since they are finely distributed through the sponge-like structure. In contrast, SEM observations conducted on the

sample processed for 20 min with the high RCQ have revealed large open cavities up to 10 µm in diameter throughout the outer oxide sublayer but no fine porosities at the top-most surface (Fig. 7). Contrary to the "sponge"-like structure that develops under the low RCQ, this "crater"-like structure presents a lower specific area and a lower charge storage capacity. In this case, right before the switching point, the accumulation of charges is therefore strong due to the combined effects of a high RCQ (low extraction of electric charges during the low magnitude of the cathodic regime) and the thinness of the inner compact oxide sublayer underneath the open cavities (Fig. 11b). This explains why the delay in the MDs appearance and the time constant of the voltage-time response remains short with the development of fewer MDs with larger size.

Interestingly, by suddenly switches the RCQ in the course of the process, the results have evidenced that the delay in the MDs appearance, the time constant of the voltage-time response and the MDs behaviour also suddenly change in opposite proportions depending on the sequenced treatment applied. If the electrical condition suddenly changes from the low RCQ to the high one, the previous oxide layer grown under the low RCQ – known to exhibit a sponge-like structure as previously discussed - is thus suddenly submitted to the high RCQ. In this case, right after the switching point, the electrical and the morphological conditions are met to promote the strongest and the most rapid accumulation of charges at the oxide / electrolyte interface. Indeed, on one hand, the dynamic of charge extraction from the surface suddenly becomes low due to the low magnitude of the cathodic current alternation, and, in other hand, the number of charges involved is high due to the high storage charge capacity of the sponge-like structure. As a consequence, and as illustrated in Fig. 11a, the MDs appears quite instantaneously with the rising edge of the anodic current that is in good agreement with the sudden drop of the delay in the MDs appearance and the time constant of the transient regime of voltage-time response. These combined effects also explain why this delay and this

time constant reached lower values than the values obtained at the same processing time within the corresponding single treatment conducted at high RCQ. In addition, when the process suddenly turns into the new RCQ, the accumulation of charge becomes so strong that it results in the development of numerous and large-size MDs. MDs are numerous due to the fact that they develop throughout the network of fine porosities at the top-most surface of the oxide layer. For a similar reason, and as illustrated in Fig. 11b, if the electrical conditions suddenly change from high to low RCQ, the mechanism of charge accumulation becomes inhibited by the combined effects of a high extraction of electric charges due to the high magnitude of the cathodic current alternation and by the limited number of charges involved in this dynamic of charge accumulation due to the lower storage capacity of the "crater"-like structure. Consequently, the dielectric breakdown is strongly delayed explaining why the delay in the MDs appearance and the time constant of the voltage-time response remains short, largely lower than the values obtained at the same processing time within the corresponding reference treatment at high RCQ (Fig. 3 and Fig. 4). Finally, for this specific sequenced treatment, the mechanism of charge accumulation is so inhibited at the oxide / electrolyte interface by the aforementioned causes that it gives rise to smoother MDs as experimentally observed (few and small-size MDs right after the switching point in Fig. 6).

4.2 PEO coatings improvement

Results clearly evidenced that the implementation of sequenced treatments have a significant effect on the coatings morphology compared to the associated reference treatments. These effects can be explained by considering the previous explanations on the relationship between the delay in the MDs appearance, the time constant τ of the voltage-time response and the MDs behaviour.

The sequenced treatment that switches from the high to the low RCQ value results in the thickest coating (109 µm) combined with a low fraction of voids (5 vol. %). Within this specific sequenced treatment, it is as if the thick overall oxide layer (~ 53 µm) formed during the first sequence (RCQ = 6.0 for 20 min in Fig. 8) is kept while the large cavities formed (up to 10 µm in diameter) are completely filled with alumina during the second sequence. These observations can be explained by considering the earlier transition into the beneficial "soft" regime during which the processed sample experiences smoother MDs regarding both their limited number over the processed surface and their smaller size (Fig. 5b). During this “soft” regime, Cheng et al. [30, 31] also proposed the ignition of internal D-type MDs that are expected to occur in the pancake-like cavities allowing these cavities to be gradually filled with solidified alumina. Said differently, the experimental results seem to support a repairing mechanism taking place inside the large cavities of the thick oxide layer elaborated during the first sequence at high RCQ. When the process switches to the low RCQ, this mechanism is suddenly triggered and, simultaneously, experimentally confirmed by the sudden changes in the MDs behaviour, the latter becoming less numerous (~ 0.28 $mm^{-2}ms^{-1}$) with smaller average size (~ 0.022 mm^2) due to the low aforementioned mechanism of charge accumulation at the oxide / electrolyte interface (Fig. 5b).

In contrast, results have shown that the reverse sequenced treatment involving the transition from the low to the high RCQ value has detrimental effects on the produced oxide layer. Indeed, although the thickness of the overall oxide layer is slightly higher than that produced with the reference treatment at low RCQ for 50 min, larger cavities are even visible throughout the coating providing a more irregular and rugged aspect of the top most surface (Fig. 8). Within this specific sequenced treatment, the preformed during the first sequence layer (RCQ = 0.9 for 20 min) is further grown, not only developing large cavities, but also at times deteriorating the previously formed compact sublayer, due to intense and large MDs. In figure 8 one can

observe that porosities have been enlarged and cracks have appeared in the sublayer of the sequenced sample (RCQ=0.9 to RCQ=6.0), compared to RCQ=0.9 for 20 min. Moreover, large cavities have been developed in the vicinity of the oxide/substrate interface, as a result of strong B-type micro-discharges, taking place throughout the total of the oxide layer. The presence of such large cavities that are usually considered as discharge channels is directly correlated with the MDs behaviour (Fig. 5). Indeed, switching from the low to the high RCQ value is associated with the sudden ignition of more numerous and larger-size MDs due to the strong aforementioned mechanism of charge accumulation at the oxide / electrolyte interface (Fig. 11).

4.3 Energy saving with PEO sequenced treatments

If a sequenced treatment starts with the high RCQ value (typ. > 1), and is then followed with the low RCQ in the range of [0.8 – 1], a thick coating with large cavities grows under strong MDs (numerous and large size MDs) during the first sequence. Then, the switching to the second sequence triggers earlier the low energy consumption "soft" regime associated with the ignition of smoother micro-discharges (less numerous and smaller size MDs). As the process goes on, the high thickness previously achieved during the first sequence is maintained and continues to grow while the large porosities are gradually filled with crystalline alumina enriched of elements from the electrolyte (mainly Si) (that could probably provide better corrosion and wear resistance). Consequently, using this virtuous sequenced treatment, the produced oxide layer is the thickest and the most compact and needs the lowest energy to grow. By this way, and as summarized in Table 1, the specific energy consumption which is defined as the electrical energy used to grow 1 µm coating over 1 m^2 proves to be the lowest (13 $kWh.m^{-2}.\mu m^{-1}$) compared to all the other treatments investigated. Particularly, by comparing with the

single treatment performed under the beneficial “soft”-regime conditions (RCQ = 0.9 during 50 min), the growth rate can be increases by ~ 40 % while maintaining a low level of porosity (~ 5 %). Interestingly, this improvement is not made at the expense of energy consumption that is actually reduced by ~ 35 %.

In contrast, if a sequenced treatment starts with the low RCQ value (0.8 < RCQ < 1) and then is followed with the high one (> 1), a thin but dense oxide layer is synthesised during the first sequence under small-size MDs. When switching to the second sequence, an “arcs” regime is triggered and more numerous and larger-size MDs are ignited. Entering into the “arcs” regime that is energy consuming, the previous dense layer developed during the first sequence is gradually damaged with the formation of large open pores that are known to degrade the wear and corrosion resistance. Therefore, and as resumed in Table 1, the specific energy consumption increases (17 $kWh.m^{-2}.\mu m^{-1}$).

4. Conclusion

The present works investigated the effects of sequenced treatments on the plasma electrolytic oxidation (PEO) of aluminium. The main conclusions are given hereafter.

- Firstly, the singular variations of the delay in the micro-discharges appearance and the time constant of the voltage-time response were explained by a mechanism of charge accumulation taking place through the electrical double layer (EDL) located at the oxide/electrolyte interface. It was established that this mechanism depends not only on the applied electrical conditions, but is also affected by the morphology of the growing oxide, particularly by the specific surface area in contact with the electrolyte.
- Secondly, a synergetic effect was observed when combining a high, at first, and a low, afterwards, ratio of charge quantity (RCQ). It resulted to a significant enhancement of the

produced coating, by increasing the total thickness and, simultaneously, maintaining a compact and dense structure of the oxide layer.

- Finally, this specific PEO sequenced treatment, despite including a high RCQ at first, resultedin a significant decrease (by ~ 35 %) in total energy consumption compared to any other treatment investigated. The use of PEO sequenced treatments opens opportunities for a better energetic management of the PEO process.

Acknowledgments

This work was supported by the French Government through the program "Investissements d'avenir" operated by the French National Research Agency (ANR) and referenced to as ANR-11-LABX-0008-01 (LabEx DAMAS).

The authors would like to acknowledge contribution of the following:

- the competence cluster on electron microscopy at IJL for providing advices in SEM observations and analyses.
- Dr. F. Brochard and APREX Solution company for their help in providing and adapting the TRACE software to our requirement for quantifying and analysing the micro-discharges.

Data availability

The data that support the findings of this study are available from the corresponding author, JM, upon reasonable request.

Contribution of each author

G.H., J.M. and A.N. conceived the experiments.

V.N. and J.M. conducted the experiments.

V.N., J.M. and A.N. performed the in-situ optical process diagnostic.

V.N. and J.M. performed all SEM analyses and interpretations. All the authors analysed the results.

V.N. and J.M. prepared the manuscript while all authors reviewed the manuscript.

J.M. and G.H. supervised the whole work.

References

[1] A.L. Yerokhin, X. Nie, A. Leyland, A. Matthews, S.J. Dowey, *Plasma electrolysis for surface engineering*, Surf. Coat. Technol. 122 (1999) 73-93.

[2] E. Matykina, A. Berkani, P. Skeldon, G.E. Thompson, *Real-time imaging of coating growth during plasma electrolytic oxidation of titanium*, Electrochim. Acta 53 (2007) 1987-1994.

[3] F. Jaspard-Mécuson, T. Czerwiec, G. Henrion, T. Belmonte, L. Dujardin, A. Viola, J. Beauvir, *Tailored aluminium oxide layers by bipolar current adjustment in the Plasma Electrolytic Oxidation (PEO) proces*s, Surf. Coat. Technol. 201 (2007) 8677-8682.

[4] J. Martin, A. Melhem, I. Shchedrina, T. Duchanoy, A. Nominé, G. Henrion, T. Czerwiec, T. Belmonte, *Effects of electrical parameters on plasma electrolytic oxidation of aluminium*, Surf. Coat. Technol. 221 (2013) 70-76.

[5] L. R. Krishna, A. S. Purnima, G. A. Sundararajan, *comparative study of tribological behavior of microarc oxidation and hard-anodized coatings*. Wear 261 (2006) 1095–1101.

[6] K. Tillous, T. Toll-Duchanoy, E. Bauer-Grosse, L. Hericher, G. Geandier, *Microstructure and phase composition of microarc oxidation surface layers formed on aluminium and its alloys 2214-T6 and 7050-T74*. Surf. Coat. Technol. 203 (2009) 2969–2973.

[7] L.O. Snizhko, A.L. Yerokhin, A. Pilkington, N.L. Gurevina, D.O. Misnyankin, A. Leyland, A. Matthews, *Anodic processes in plasma electrolytic oxidation of aluminium in alkaline solutions*, Electrochim. Acta 49 (2004) 2085-2095.

[8] H. F. Guo, M.Z. An, H.B. Huo, S. Xu, L.J. Wu, *Microstructure characteristic of ceramic coatings fabricated on magnesium alloys by micro-arc oxidation in alkaline silicate solution*, Appl. Surf. Sci 252 (2006) 7911-7916.

[9] Q. Cai, L. Wang, B. Wei, Q. Liu, *Electrochemical performance of microarc oxidation films formed on AZ91D magnesium alloy in silicate and phosphate electrolytes*, Surf. Coat. Technol. 200 (2006) 3727-3733.

[10] C. Blawert, V. Heitmann, W. Dietzel, H.M. Nykyforchyn, M. Klapkiv, *Influence of electrolyte on corrosion properties of plasma electrolytic conversion coated magnesium alloys*, Surf. Coat. Technol. 201 (2007) 8709-8714.

[11] J. Liang, P. Bala Srinivasan, C. Blawert, M. Störmer, W. Dietzel, *Electrochemical corrosion behaviour of plasma electrolytic oxidation coatings on AM50 magnesium alloy formed in silicate and phosphate based electrolytes*, Electrochim. Acta 54 (2009) 3842-3850.

[12] A.L. Yerokhin, A. Shatrov, V. Samsonov, P. Shashkov, A. Pilkington, A. Leyland, A. Matthews, *Oxide ceramic coatings on aluminium alloys produced by a pulsed bipolar plasma electrolytic oxidation process*, Surf. Coat. Technol. 199 (2005) 150-157.

[13] E. Matykina, R. Arrabal, P. Skeldon, G.E. Thompson, *Investigation of the growth processes of coatings formed by AC plasma electrolytic oxidation of aluminium*, Electrochim. Acta 54 (2009) 6767-6778.

[14] E.V. Parfenov, A. Yerokhin, A. Matthews, *Small signal frequency response studies for plasma electrolytic oxidation*, Surf. Coat. Technol. 203 (2009) 2896-2904.

[15] P. Bala Srinivasan, J. Liang, R.G. Balajeee, C. Blawert, M. Störmer, W. Dietzel, *Effect of pulse frequency on the microstructure, phase composition and corrosion performance of a phosphate-based plasma electrolytic oxidation coated AM50 magnesium alloy*, Appl. Surf. Sci. 256 (2010) 3928-3935.

[16] A. Melhem, G. Henrion, T. Czerwiec, J.L. Briançon, T. Duchanoy, F. Brochard, T. Belmonte, *Changes induced by process parameters in oxide layers grown by the PEO process on Al alloys*, Surf. Coat. Technol. 205 (2011) S133-S136.

[17] R.O. Hussein, D.O. Northwood, X. Nie, *The influence of pulse timing and current mode on the microstructure and corrosion behaviour of a plasma electrolytic oxidation (PEO) coated AM60B magnesium alloy*, J. Alloys Comp. 541 (2012) 41-48.

[18] A. V. Timoshenko and Y. V. Magurova, *Investigation of plasma electrolytic oxidation processes of magnesium alloy MA2-1 under pulse polarisation modes*, Surf. Coat. Technol., 199 (2005) 135–140.

[19] J. Martin, A. Nominé, F. Brochard, J-L. Briançon, C. Noël, T. Belmonte, T. Czerwiec, G. Henrion, *Delay in micro-discharges appearance during PEO of Al: Evidence of a mechanism of charge accumulation at the electrolyte / oxide interface*. Appl. Surf. Sci. 410 (2017) 29-41.

[20] M.D. Klapkiv, *State of an electrolytic plasma in the process of synthesis of oxides based on aluminum*, Mater. Sci. 31 (1996) 494-499.

[21] M.D. Klapkiv, *Simulation of synthesis of oxide-ceramic coatings in discharge channels of a metal-electrolyte system*, Mater. Sci. 35 (1999) 279-283.

[22] G. Sundararajan, L. Rama Krishna, *Mechanisms underlying the formation of thick alumina coatings through the MAO coating technology*, Surf. Coat. Technol. 167 (2003) 269-277.

[23] L.R. Krishna, A.S. Purnima, N.P. Wasekar, G. Sundararajan, *Kinetics and Properties of Micro Arc Oxidation Coatings Deposited on Commercial Al Alloys*, Metall. Mater. Trans. A 38 (2007) 370-378.

[24] A.L. Yerokhin, V.V. Lyubimov, R.V. Ashitkov, *Phase formation in ceramic coatings during plasma electrolytic oxidation of aluminium alloys*, Ceram. Int. 24 (1998) 1-6.

[25] E. Matykina, R. Arrabal, D.J. Scurr, A. Baron, P. Skeldon, G.E. Thompson, *Investigation of the mechanism of plasma electrolytic oxidation of aluminium using ^{18}O tracer*, Corr. Sci. 52 (2010) 1070-1076.

[26] R.O. Hussein, X; Nie, D.O. Northwood, A. Yerokhin, A. Matthews, *Spectroscopic study of electrolytic plasma and discharging behaviour during the plasma electrolytic oxidation (PEO) process*, J. Phys. D.: Appl. Phys. 43 (2010) 105203.

[27] R.O. Hussein, X. Nie, D.O. Northwood, *An investigation of ceramic coating growth mechanisms in plasma electrolytic oxidation (PEO) processing*, Electrochim. Acta 112 (2013) 111-119.

[28] J. Jovović, S. Stojadinović, N.M. Šišović, N. Konjević, *Spectroscopic characterization of plasma during electrolytic oxidation (PEO) of aluminium*, Surf. Coat. Technol. 206 (2011) 24-28.

[29] V. Dehnavi, B.L. Luan, D.W. Shoesmith, X.Y. Liu, S. Rohani, *Effect of duty cycle and applied current frequency on plasma electrolytic oxidation (PEO) coating growth behaviour*, Surf. Coat. Technol. 226 (2013) 100-107.

[30] Y. Cheng, F. Wu, E. Matykina, P. Skeldon, G.E. Thompson, *The influences of microdischarge types and silicate on the morphologies and phase compositions of plasma electrolytic oxidation coatings on Zircaloy-2*, Corr. Sci. 59 (2012) 307-315.

[31] Y. Cheng, Z. Xue, Q. Wang, X. Wu, E. Matykina, P. Skeldon, G.E. Thompson, *New findings on properties of plasma electrolytic oxidation coatings from study of an Al–Cu–Li alloy*, Electrochim. Acta 107 (2013) 358-378.

[32] Y. Cheng, M. Mao, J. Cao, Z. Peng, *Plasma electrolytic oxidation of an Al-Cu-Li alloy in alkaline aluminate electrolytes: A competition between growth and dissolution for the initial ultra-thin films*, Electrochim. Acta 138 (2014) 417-429.

[33] A. Nominé, A. V. Nominé, N. St. J. Braithwaite, T. Belmonte, G. Henrion, *High-Frequency-Induced Cathodic Breakdown during Plasma Electrolytic Oxidation*, Phys. Rev. Appl. 8 (2017) 031001.

[34] A. B. Rogov, A. Yerokhin, A. Matthews, *The role of cathodic current in plasma electrolytic oxidation of aluminum: Phenomenological concepts of the "soft sparking" mode*, Langmuir, 33 (2017), 11059 – 11069.

[35] A.B. Rogov, V.R. Shayapov, *The role of cathodic current in PEO of aluminium: influence of cationic electrolyte composition on the transient current voltage curves and the discharges optical emission spectra*, Appl. Surf. Sci. 394 (2017) 323-332.

[36] S. Bardin, J-L. Briançon, F. Brochard, V. Martin, Y. Zayachuk, R. Hugon, J. Bougdira, *Investigating transport of dust particles in plasmas*, Contrib. Plasma Phys. 51 (2011) 246-251.

[37] N. Endstrasser, F. Brochard, V. Rohde, M. Balden, T. Lunt, S. Bardin, J.-L. Briançon, R. Neu, *Video tracking and post-mortem analysis of dust particles from all tungsten ASDEX* Upgrade, J. Nucl. Mater. 415 (2011) S1085-S1088.

[38] A. Nominé, J. Martin, C. Noël, G. Henrion, T. Belmonte, I.V. Bardin, P. Lukès, *Surface charge at the oxide/electrolyte interface: Toward optimization of electrolyte composition for treatment of Aluminum and Magnesium by Plasma Electrolytic Oxidation*, Langmuir 32 (2016) 1405–1409.

[39] V. Dehnavi, D. W. Shoesmith, B. L. Luan, M. Yarid, X. Y. Liu, S. Rohani, *Corrosion properties of plasma electrolytic oxidation coatings on an aluminium alloy – The effect of the PEO process stage*, Mater. Chem. Phys. 161 (2015) 49-58.

[40] A. Ghasemi, V.S. Raja, C. Blawert, W. Dietzel, K.U. Kainer, *The role of anions in the formation and corrosion resistance of the plasma electrolytic oxidation coatings*, Surf. Coat. Technol. 204 (2009) 1469-1478.

[41] A. Polat, M. Makaraci, M. Usta, *Influence of sodium silicate concentration on structural and tribological properties of microarc oxidation coatings on 2017A aluminum alloy substrate*, J. Alloys Comp. 504 (2010) 519-526.

List of tables

Table 1: Parameters of current waveforms used for RCQ = 0.9 and RCQ = 6

RCQ	Q_p (mC)	Q_n (mC)	Waveform
0.9	61	68.4	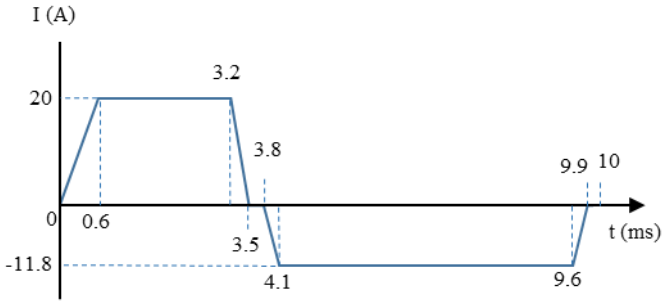
6	61	10.4	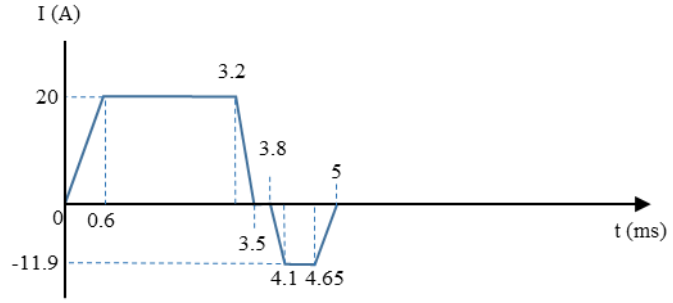

Table 2: PEO treatments performed with the associated time of the "soft" regime appearance, the average thickness and the porosity of the overall PEO coatings and the specific energy consumption.

	First sequence from 0 to 20 min	**Second sequence from 20 to 50 min**	**t_{SR}* (± 1 min)**	**Overall Thickness (± 5 µm)**	**Void fraction (± 3 %)**	**Specific Energy Consumption (± 1 kWh.m^{-2}·µm^{-1})**
Reference treatments	RCQ** = 0.9	-	-	35	7	12
	RCQ = 6.0	-	-	53	15	13
	RCQ = 0.9	RCQ = 0.9	30	62	3	17
	RCQ = 6.0	RCQ = 6.0	-	70	13	25
Sequenced treatments	RCQ = 0.9	RCQ = 6.0	-	76	12	15
	RCQ = 6.0	RCQ = 0.9	23	109	5	11

*t_{SR} = Time of the "soft" regime appearance

** RCQ = Charge Quantity Ratio

List of figures

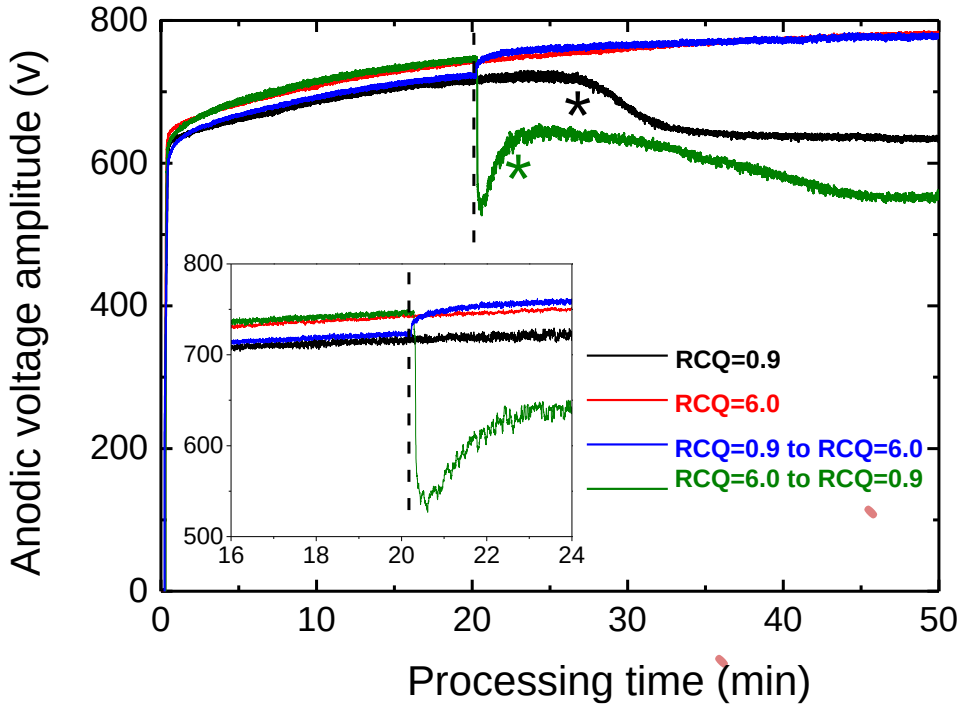

Figure 1: Time evolution of the anodic voltage amplitude for the different conditions investigated and summarized in Table 1. The vertical dash line (---) indicates the switching time of the RCQ conditions. Stars (*) indicate the time at which the process enters into the "soft" regime.

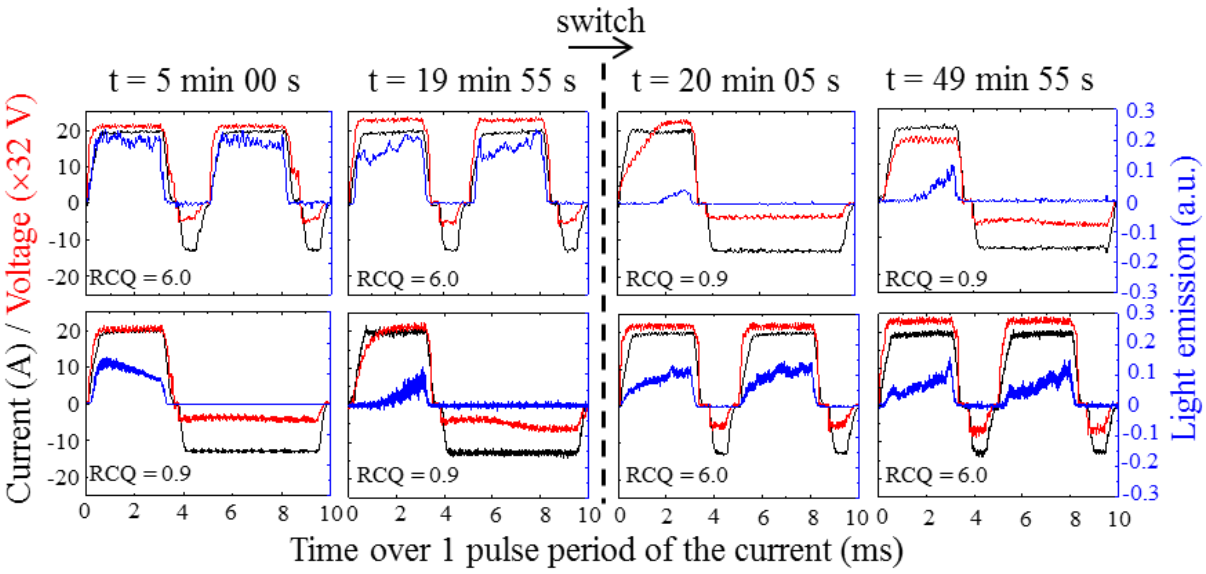

Figure 2: Evolution of the light emission (blue lines) with the corresponding current (black lines) and voltage (red lines) signals recorded over 10 ms for the sequenced PEO treatments investigated and summarized in Table 1. The vertical dash line (---) indicates the switching time of the RCQ conditions.

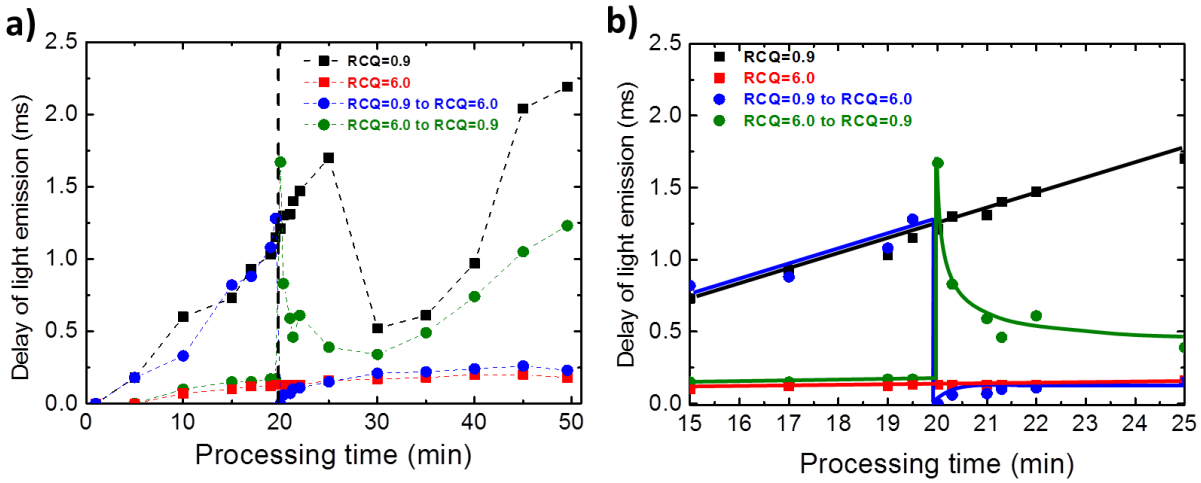

Figure 3: a) Evolution of the delay of light emission as a function of processing time for the different PEO processing conditions investigated and summarized in Table 1. The vertical dash line (---) indicates the switching time of the RCQ conditions. b) Close-up of the delay evolution close to the switching time at 20 min.

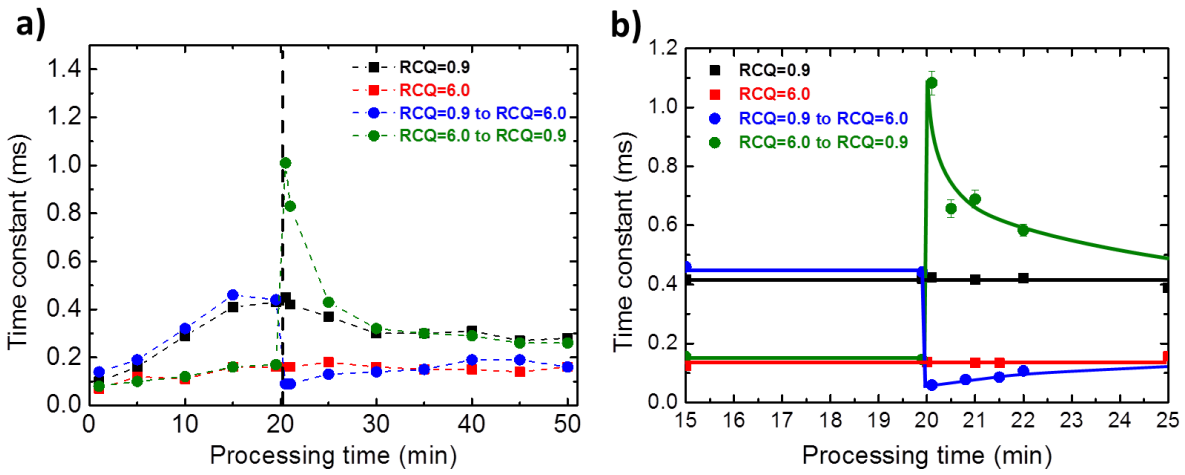

Figure 4: a) Evolution of the time constant of the anodic voltage transient as a function of processing time for the different PEO processing conditions investigated and summarized in Table 1. The vertical dash line (---) indicates the switching time of the RCQ conditions. b) Close-up of the time constant evolution close to the switching time at 20 min.

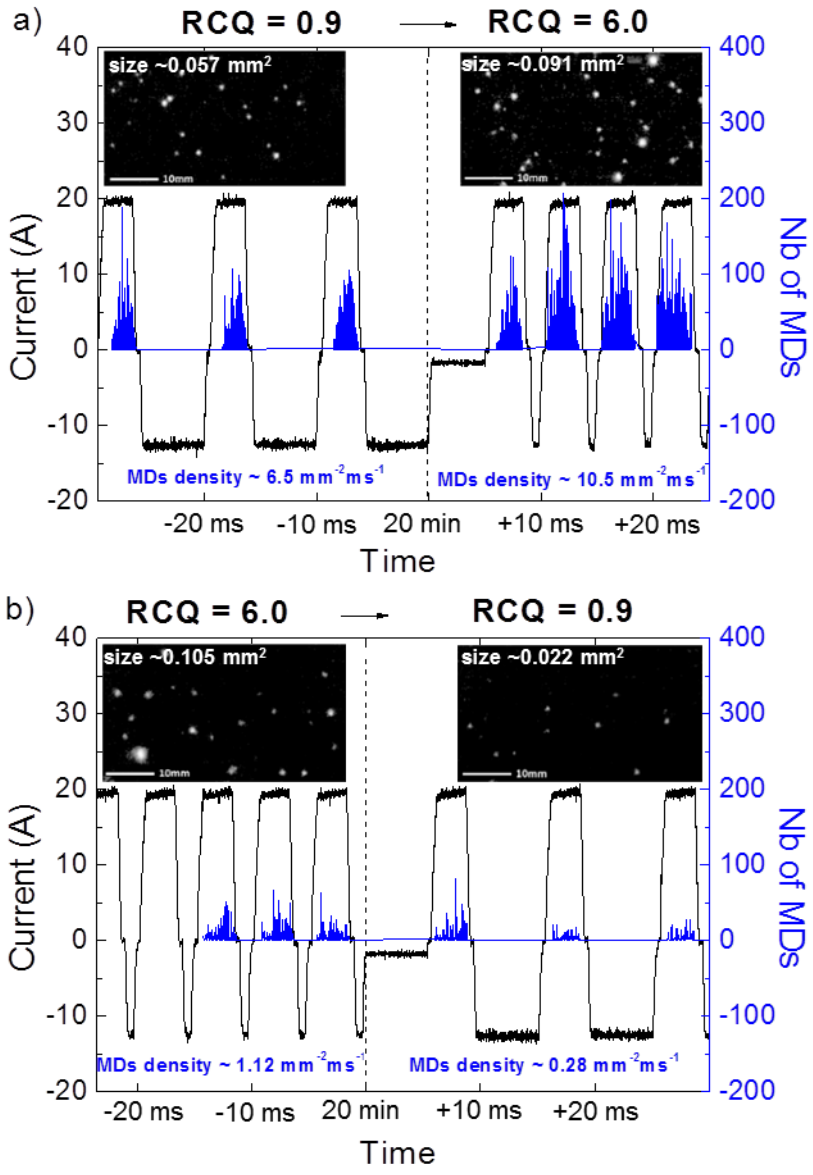

Figure 5: Evolution of the number of the micro-discharges (blue lines) that were detected using fast video imaging with the corresponding current signal (black lines) recorded exactly when the PEO process switches from one RCQ to the second one (see Table 1). The vertical dash line (---) indicates the switching time of the RCQ conditions. The insets are frames captured from the movie of the processed sample recorded with fast video camera. a) For the sequenced treatment that switches from the low RCQ = 0.9 to the high RCQ = 6.0. b) For the sequenced treatment that switches from the high RCQ = 6.0 to the low RCQ = 0.9.

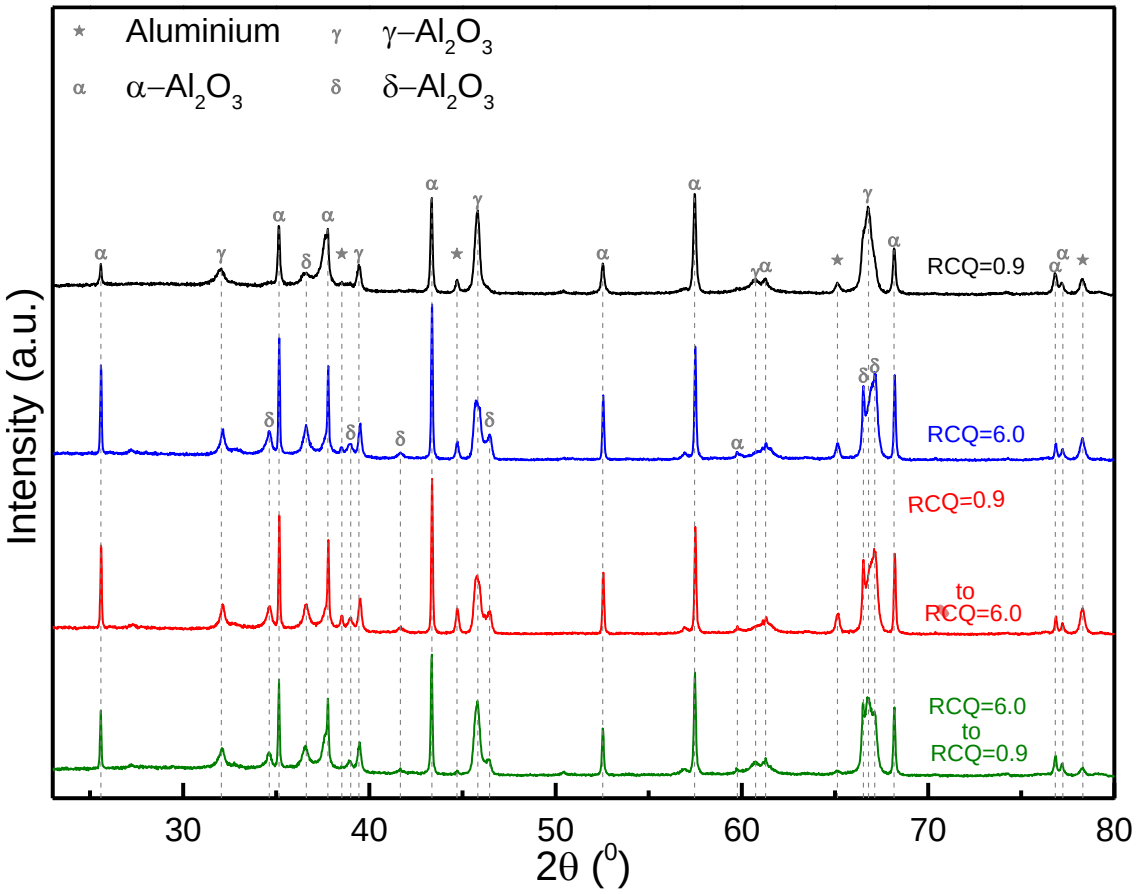

Figure 6: XRD patterns of the oxide coatings produced under different conditions. Bragg-Brentano θ/2θ configuration, λ=1,5406 Å.

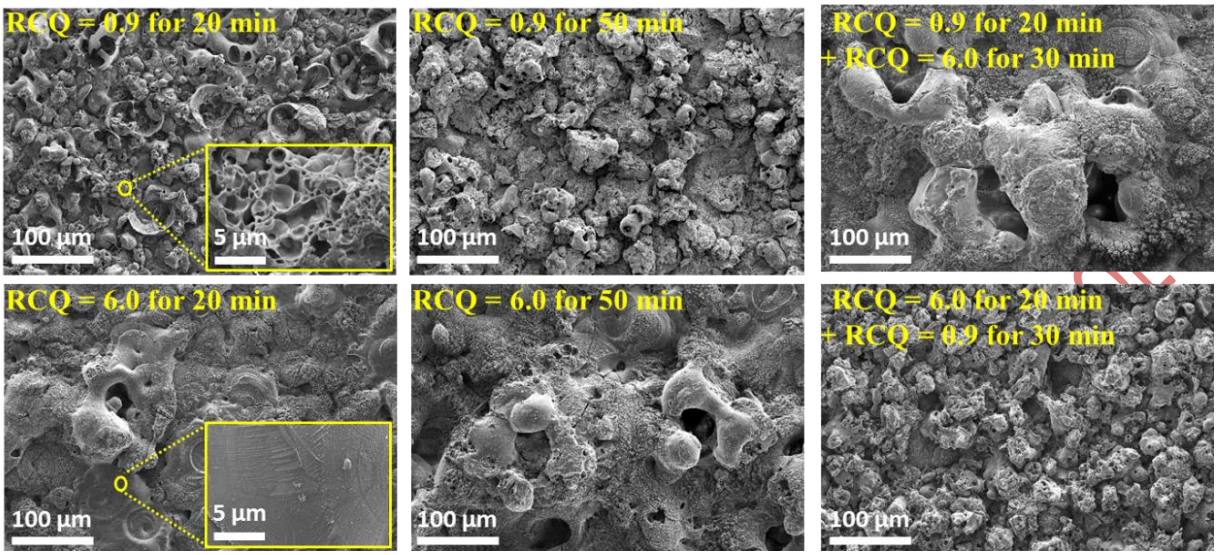

Figure 7: SEM top-surface views of the PEO oxide layers elaborated under the different PEO processing conditions investigated and summarized in Table 1.

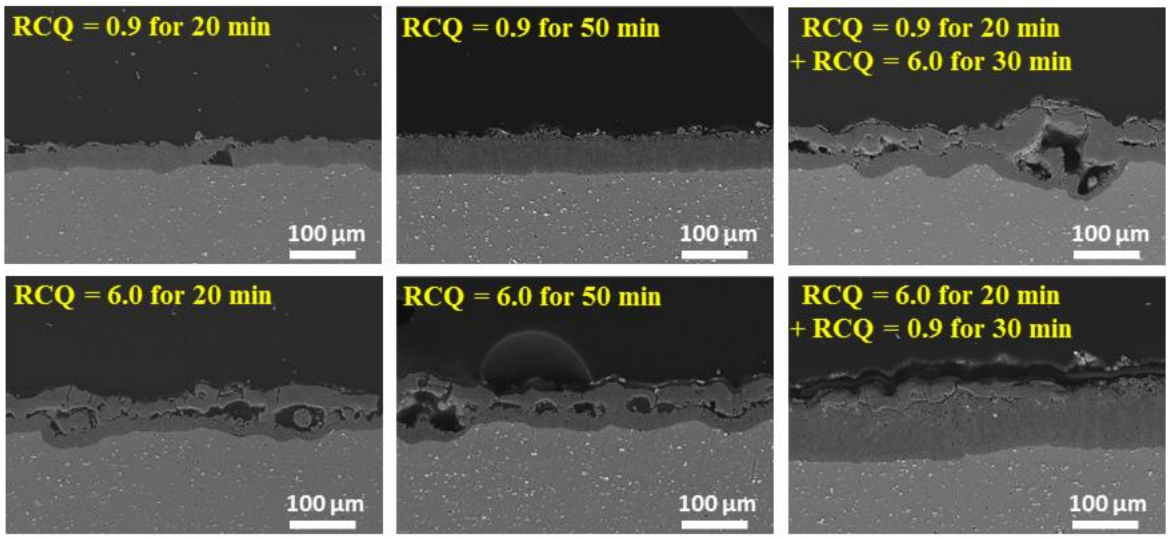

Figure 8: SEM cross-sectional views of the PEO oxide layers elaborated under the different PEO processing conditions investigated and summarized in Table 1.

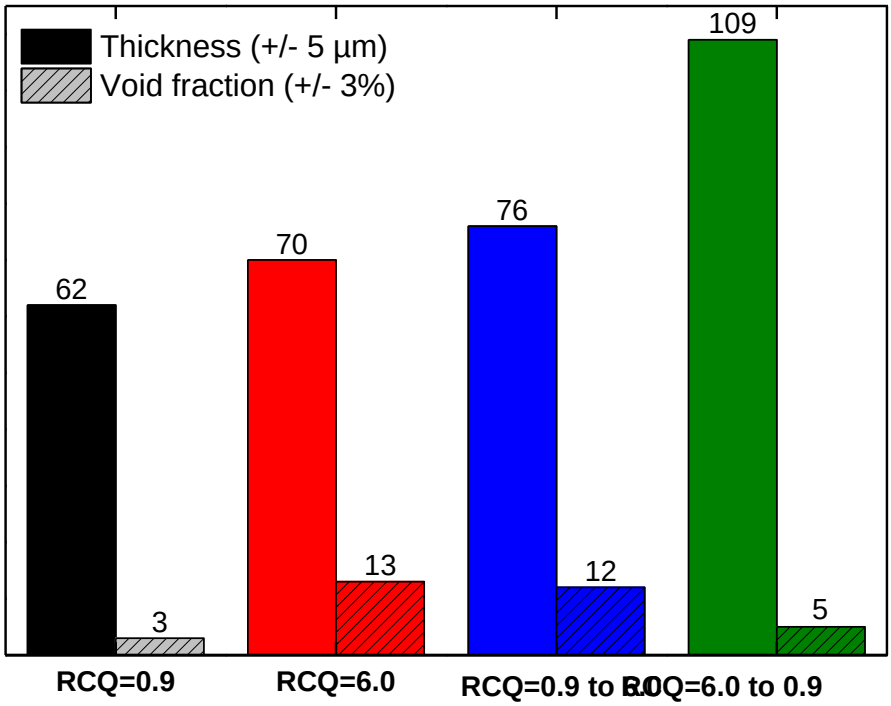

Figure 9: Measured thickness and estimated void fraction of the PEO oxide layers elaborated for 50 min under the different PEO processing conditions investigated and summarized in Table 1.

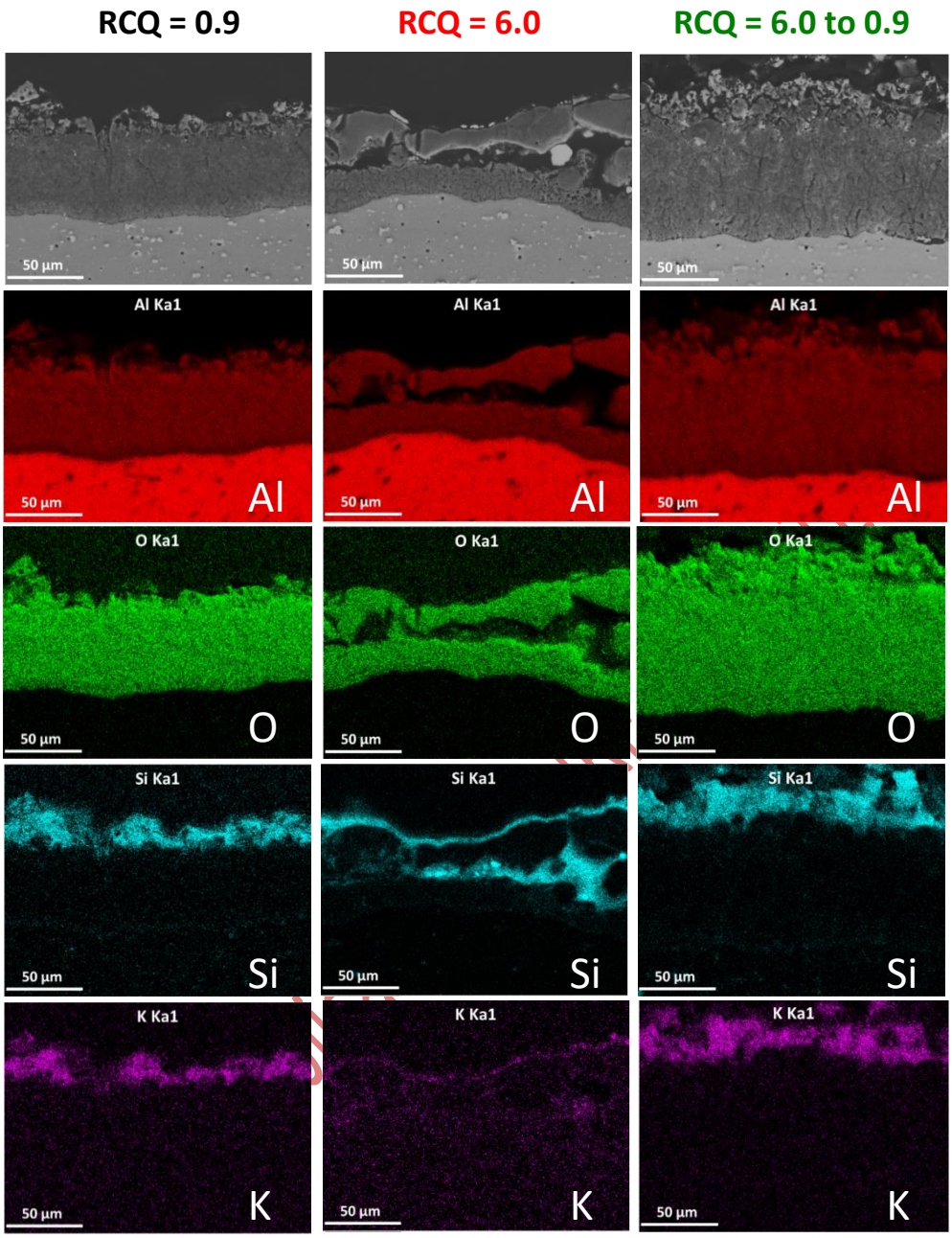

Figure 10: SEM cross-sectional views and the associated EDX element maps (Al, O, Si and K) of the PEO oxide layers elaborated for 50 min with the reference treatments (RCQ = 0.9 and RCQ = 6.0) and with the sequenced treatment (RCQ = 6.0 for 20 min followed with RCQ = 0.9 for 30 min)

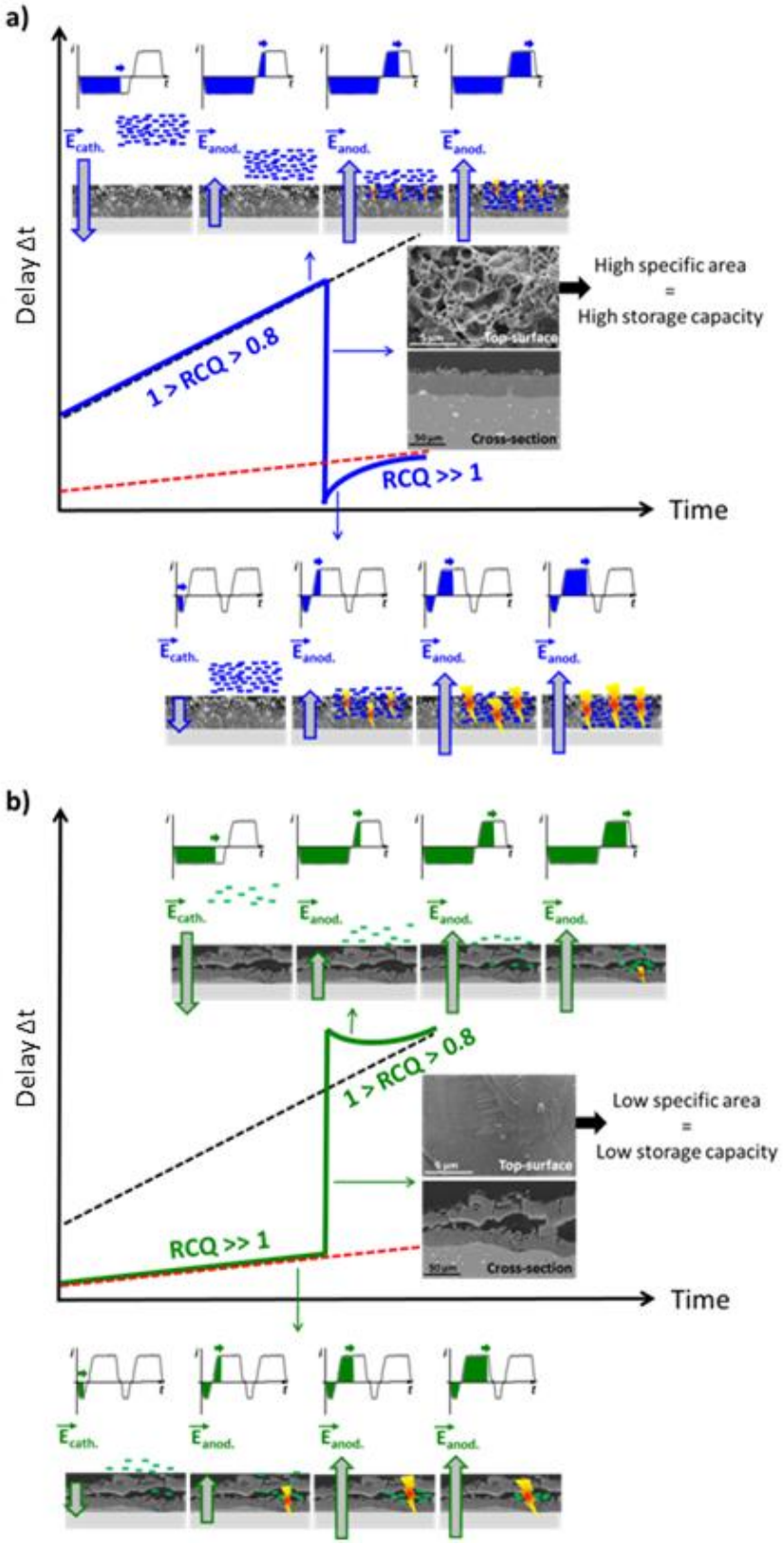

Figure 11: Schematic model of combined effects of the ratio of charge quantity (RCQ) and the coating morphology on the micro-discharges properties exactly when the PEO process

suddenly switches a) from a high RCQ (RCQ = 6.0) to a low RCQ (RCQ = 0.9) (blue line) and b) for the reverse sequence (green line).